

# Organically Modified Titania–Silica Aerogels for the Epoxidation of Olefins and Allylic Alcohols

C. A. Müller, M. Maciejewski, T. Mallat, and A. Baiker<sup>1</sup>

Laboratory for Technical Chemistry, Swiss Federal Institute of Technology, ETH Zentrum, CH-8092 Zurich, Switzerland

Received November 21, 1998; revised January 12, 1999; accepted January 12, 1999

Mesoporous titania–silica mixed oxides with varying amounts of covalently bound methyl groups were prepared from methyltrimethoxysilane and tetramethoxysilane using a sol-gel process and ensuing low temperature supercritical extraction with CO<sub>2</sub>. The aerogels containing 20 wt% TiO<sub>2</sub> were characterized by thermal analysis, N<sub>2</sub> and NH<sub>3</sub> adsorption, infrared spectroscopy, NMR, X-ray photoelectron spectroscopy, and transmission electron microscopy. The amorphous mesoporous structure of the aerogels did not depend markedly on the amount of modifier. The titania dispersion within the silica matrix was slightly lowered for methyl-modified materials. <sup>29</sup>Si CP-MAS NMR measurements indicated a more cross-linked network for the unmodified catalyst. Methyl groups located at the surface replaced part of the silanol groups present in the unmodified aerogel, resulting in a decreased ability to adsorb ammonia. The modified aerogels showed high thermal stability: a significant rate of Si–C bond breaking was detected only above 400°C. The materials were tested in the epoxidation of various olefins and allylic alcohols. The olefin epoxidation activity was generally lowered by the methyl modification, whereas in the epoxidation of allylic alcohol a maximum in activity was observed with increasing methyl content. In the epoxidation of cyclohexenol, 98% selectivity at 90% conversion was achieved in 10 min. Dependent on their basicity, inorganic salts and bases as additives exhibited a strong influence on the reaction over modified aerogels. This behavior is suggested to be due to: (i) different titanium complexes which form upon interaction with the reactant and basic additive and (ii) the resulting change of the stability/reactivity of the peroxo-titanium complex. © 1999 Academic Press

**Key Words:** titania–silica aerogel; epoxidation; olefin; allylic alcohol; <sup>29</sup>Si CP-MAS; NMR; pulse thermal analysis; infrared spectroscopy; transmission electron microscopy.

## 1. INTRODUCTION

Considerable efforts have been made for developing solid materials capable of catalyzing the epoxidation of olefins (1, 2). The most efficient catalysts are Ti- and Si-containing materials, including various titania–silicas and

Ti-substituted zeolites. Two types of titania–silica catalysts have been intensively investigated, silica-supported titania (Shell catalyst) (3) and mesoporous titania–silica mixed oxides (4–7). Titania–silica mixed oxides based on the sol-gel method (8) may exhibit better titanium distribution throughout the silica matrix when compared to the Shell catalyst. Titania–silica aerogels prepared by the sol-gel method and supercritical drying with CO<sub>2</sub> (9) proved to be extremely active and selective for a variety of bulky cyclic alkenes, alkenones, and alkenols (4, 5, 7, 10). The mesoporous structure and well-dispersed titanium in the silica matrix were identified as major prerequisites for good catalytic performance. However, the catalyst was deactivated by aqueous hydrogen peroxide due to leaching of the active titanium species (5).

Leaching of Ti in an aqueous medium was explained by the hydrophilicity of common titania–silica mixed oxides (11). The hydrophilic character of these catalysts has become a subject of interest, and just recently Klein and Maier (12) and Kochkar and Figueras (11) prepared organically modified microporous and mesoporous mixed oxides, respectively. The primary aim was to enable the use of aqueous hydrogen peroxide. Hydrophobization of the surface was achieved by substituting a fraction of the surface silanol groups by methyl or phenyl groups covalently bound to Si. Partial substitution of the tetraethoxysilane precursor by methyltriethoxysilane or phenyltriethoxysilane afforded stable catalysts for the epoxidation of olefins with hydrogen peroxide. However, the catalytic activities and selectivities observed when using aqueous H<sub>2</sub>O<sub>2</sub> as oxidant were still low compared to the reaction with TBHP in organic medium (11). The moderate performance of organically modified titania–silica in a facile reaction such as the epoxidation of cyclohexene indicates that these materials are not suitable for reactions in the presence of water. Apparently, the hydrophilicity of titania–silica is not the most important characteristic different from TS-1, whose molecular sieve material represents the best epoxidation catalyst, efficient in an aqueous medium.

Modification of titania–silica by covalently bound organic functional groups could also be a valuable tool for

<sup>1</sup> To whom correspondence should be addressed. Fax: +41 1 632 11 63; E-mail: a.baiker@tech.chem.ethz.ch.

adjusting the structural properties to the requirements of the epoxidation reactions. The potential of organic modification of silica is reflected by a wealth of data demonstrating a multitude of beneficial applications (13–24).

The present study aimed at investigating the influence of organic surface modification on the catalytic behavior of a mesoporous aerogel in the epoxidation of various linear and cyclic olefins and allylic alcohols with TBHP. Desired features of the aerogel catalysts were (i) well-dispersed Ti in the silica matrix, (ii) a mesoporous structure providing access for bulky reactants to the active sites, and (iii) covalently anchored organic functional groups stable under the conditions of catalyst preparation and epoxidation reaction.

## 2. EXPERIMENTAL

### Catalyst Preparation

The aerogels were prepared based on a procedure previously published (9). Conditions of the various preparations are listed in Table 1. The abbreviation Ae stands for aerogel. The numbers before these letters denominate the percentage of modified silicon precursor related to the total amount of silicon. If no additional information is given, the prehydrolysis time was 6 h, whereas differing prehydrolysis times are specified, e.g., 30Ae–12 h. The sol-gel process was carried out in a glass reactor at ambient temperatures under a He atmosphere. The total volume of the liquid was ca. 170 ml and the corresponding molar ratios of water : silicon alkoxide : acid were 5 : 1 : 0.1.

The lower reactivity of the methyltrimethoxysilane (MTMS; Fluka, puriss.) precursor compared to tetramethoxysilane for hydrolysis and condensation (8) required a prehydrolysis step. This step was carried out in 22 ml of *i*-propanol (*i*-PrOH) by adding the hydrolysant, consisting of 750 mmol water (distilled after ion exchange) and 15 mmol

acid (HNO<sub>3</sub> 65%; Fluka, puriss.) diluted in 40 ml *i*-PrOH, to the MTMS according to Table 1. The solution was vigorously stirred (ca. 1000 rpm) for the corresponding prehydrolysis time (Table 1) under inert atmosphere. Then, the remaining constituents, tetramethoxysilane (TMOS; Fluka, puriss.) and 28.1 mmol titanbisacetylacetonatdiisopropoxide (TIBADIP, 75% in *i*-PrOH; Aldrich puriss.) in 10 ml *i*-PrOH, were added. The remaining alcohol (50 ml) was added after 5 min and the stirring speed reduced (ca. 500 rpm). Gelation to an opaque monolithic body occurred within 24 h.

Semicontinuous extraction with supercritical CO<sub>2</sub> was carried out at 40°C and 230 bar. A glass liner was used to prevent leaching of components from the steel autoclave. The as-prepared aerogel clumps were ground in a mortar and calcined in a tubular reactor with upward flow. About 2 g samples were heated to 400°C at 10°C min<sup>-1</sup> in an air flow of 5 l min<sup>-1</sup> and kept at this temperature for 1 h.

The composition of the samples with regard to Si, Ti, and Fe was determined by inductively coupled plasma atomic emission spectroscopy (ICPAES). The Si and Ti contents were nominal within the range of the experimental error and the Fe content was below 0.01% (detection limit).

### Thermal Analysis

Experiments were carried out on a Netzsch STA 409 thermoanalyzer equipped with a gas injector. Gases evolved during reaction and/or injected into the system were monitored on-line with a Balzers QMG 420 quadrupole mass spectrometer, connected to the thermoanalyzer by a heated (ca. 200°C) capillary.

Ammonia adsorption was measured at 50°C. Prior to the adsorption, the sample was heated under helium to 200°C and kept at this temperature for 1 h to remove the adsorbed molecules, mainly water and carbon dioxide. After cooling to 50°C, 0.5-ml pulses of ammonia were injected into the stream of helium (50 ml/min). The mass of the sample was in the range of 40–50 mg. Progress of the adsorption was monitored by the change of the sample mass (thermogravimetric curve, TG) with an accuracy of a few μg. Generally, the first three pulses of ammonia were adsorbed irreversibly, the ammonia injected in next pulses was physisorbed, and its desorption occurred after ca. 100 min. After complete desorption of weakly physisorbed ammonia, the next pulse(s) was injected to confirm the occurrence of the physisorption process only. More details of this new method will be published elsewhere (25).

Immediately after completing the adsorption experiment, the sample was heated with a rate of 10°C/min under helium (50 ml/min) from 50 to 600°C. Ammonia desorption was monitored by TG and MS analysis ( $m/z = 15$  and 17). The MS signal of NH<sub>3</sub> at  $m/z = 15$  overlapped with that of CH<sub>3</sub> fragments evolved from the aerogels at temperatures above 300°C.

TABLE 1

Quantities and Prehydrolysis Times for Sol-Gel Preparations

Aerogel <sup>a</sup>	MTMS <sup>b</sup> mmol	TMOS <sup>c</sup> mmol	Prehydrolysis time h
0Ae	0	150	6
10Ae	15	135	6
20Ae	30	120	6
30Ae <sup>d</sup>	45	105	6
30Ae–12h	45	105	12
30Ae–24h	45	105	24

<sup>a</sup> The number before the letters designates the fraction to methyltrimethoxysilane related to the total amount of silane (MTMS + TMOS).

<sup>b</sup> Methyltrimethoxysilane.

<sup>c</sup> Tetramethoxysilane.

<sup>d</sup> Corresponds to "30Ae–6h."

Quantification of the methyl content was based on its partial oxidation during calcination of the samples under oxygen (80 vol% O<sub>2</sub> in helium). In helium, the evolution of CH<sub>3</sub> species, indicated by the MS signal of  $m/z = 15$ , was observed in the range of 300–950°C (heating rate 10°C/min). A negligible amount of CO<sub>2</sub> ( $m/z = 44$ ) formed due to the oxidation of carbon containing species by traces of oxygen present in the system was detected as well. In oxygen, the major part of the CH<sub>3</sub> species was oxidized to CO<sub>2</sub> and water. The amount of CO<sub>2</sub> formed was determined by comparing the integral intensity of its characteristic MS signal ( $m/z = 44$ ) with the calibration signals produced by the injection of 0.5-ml pulses of CO<sub>2</sub> (details of the applied method of MS signal quantification are described elsewhere (26, 27)). The amount of covalently bound CH<sub>3</sub> groups was calculated from the balance of the carbon present in CH<sub>3</sub> and CO<sub>2</sub> detected in experiments under helium and oxygen, respectively (25).

### Nitrogen Physisorption

The specific surface areas ( $S_{\text{BET}}$ ), mean cylindrical pore diameters ( $\langle d_p \rangle$ ), and specific desorption pore volumes ( $V_p(\text{N}_2)$ ), assessed by the BJH method, were determined by nitrogen physisorption at –196°C using a Micromeritics ASAP 2000 instrument. Prior to measurement, the samples were degassed at 100°C until a final constant pressure below 0.1 Pa was achieved. BET surface areas were calculated in a relative pressure range between 0.05 and 0.2, assuming a cross-sectional area of 0.162 nm<sup>2</sup> for the nitrogen molecule. The pore size distributions were calculated applying the BJH method to the desorption branches of the isotherms (28). The fractal dimensions of the surface structure were calculated according to Jarzebski *et al.* (29).

### FTIR Transmission Spectroscopy

FTIR measurements were performed on a Perkin Elmer series 2000 instrument. Sample wafers consisted of 100 mg dry KBr and ca. 1 mg calcined sample. The sample cell was purged with a small flow of oxygen during the measurements. Then, 500 scans were accumulated for each spectrum, at a spectral resolution of 4 cm<sup>-1</sup>.

The calculation of the approximate Ti dispersion was estimated using

$$R = \frac{S_{(\text{Si-O-Ti})}}{S_{(\text{Si-O-Si})}} \quad [1]$$

where  $S_{(\text{Si-O-Ti})}$  is the deconvoluted area of the peak at ca. 940 cm<sup>-1</sup> and  $S_{(\text{Si-O-Si})}$  that at ca. 1210 cm<sup>-1</sup>. The procedure has been described in a previous study (9).

### DRIFT Spectroscopy

Diffuse reflectance infrared Fourier transform (DRIFT) spectroscopy was carried out on a Perkin Elmer series 2000 instrument. The samples were prepared by mixing the aero-

gel material (ca. 10 mg) with dry KBr (90 mg). Each sample was preheated in air to 250°C with a heating rate of 5°C min<sup>-1</sup>. After cooling to 50°C, the background spectra were recorded at temperatures of 50, 100, 150, 200, and 250°C under air, applying the same temperature program as before. The spectra were accumulated from 20 scans in a range of 10°C (e.g., 95–105°C). The sample was flushed at 50°C with Ar (0.5 h), then with NH<sub>3</sub> (5% in Ar) for 0.5 h. Subsequently, the atmosphere was switched again to Ar for 1.5 h. After recording the DRIFT spectrum, the temperature programmed desorption spectra were measured at temperatures of 50, 100, 150, 200, and 250°C in Ar, applying the same temperature program as before. The DRIFT difference spectra were obtained by subtracting the corresponding background spectra from the temperature programmed desorption (TPD) spectra.

### NMR Spectroscopy

For the deconvolution of the T<sup>2</sup>, T<sup>3</sup>, Q<sup>2</sup>, Q<sup>3</sup>, and Q<sup>4</sup> CP/MAS signals, starting values of –56, –64, –92, –100, and –109 ppm, respectively, were chosen. The peak positions and the width of the peaks were not fixed. A Gaussian function was chosen as a fitting function. The fit was optimized using the least squares method.

The relation given in Eq. [2] for the pulse time-dependent magnetization  $M(t)$  (30) was used to fit the experimental data obtained from the deconvolution with six adjustable parameters,

$$M(t) = \frac{M_0}{1 - \lambda} \times \left[ e^{-\frac{t}{T_{1\rho}}} - a e^{-\frac{t}{T_{1s}}} - (1 - a) \left[ \left( \frac{1}{2} e^{-\frac{t}{T_{11}}} + \frac{1}{2} e^{-\frac{3t}{2T_{11}}} \cos \frac{1}{2} bt \right) \right] \right] \quad [2]$$

Where no decrease in magnetization could be observed,  $T_{1\rho}$  was set equal to infinity. When no convergence could be reached, the values of parameters as indicated in the text were set constant to facilitate convergence. In these cases, a manual optimization of the fixed parameters was performed to minimize errors.

### XPS

XPS spectra were obtained using a Leybold LHS 11 instrument. Mg K<sub>α</sub> radiation (240 W) was applied to excite photoelectrons, which were detected with the analyzer operated at 38 eV constant pass energy. Corrections of the energy shift were accomplished taking the C 1s line at 285.0 eV.

### Electron Microscopy

For the TEM investigation, the sample was crushed and deposited on a holey carbon foil supported by a copper grid. The Philips CM30 microscope, operated at 300 kV, was equipped with a Supertwin lens ( $cs = 1.2$  mm, point resolution < 0.2 nm).

### Catalytic Tests

*Trans*-2-hexen-1-ol (Aldrich, 96%), cinnamyl alcohol (Fluka, >97%), 2-cyclohexen-1-ol (Fluka, ca. 97%), 1-hexene (Fluka, >98%), isophorone (Fluka, >97%), cyclohexene (Fluka, >99.5%), and *tert*-butylhydroperoxide (TBHP; Fluka, ca. 5.5 M solution in nonane, stored over molecular sieve 4 Å) were used as received. Toluene (Riedel-de Haën, >99.7%) was distilled and stored over a molecular sieve. Molecular sieve 4 Å (Chemie Uetikon) was activated overnight at 200°C for 24 h.

All reactions were carried out under purified He to avoid the presence of oxygen and moisture. In the standard procedure, 250-mg catalyst was transferred to a 200-ml glass reactor, equipped with a mechanical stirrer, thermometer, and reflux condenser, and heated in a He flow to 200°C for 2 h. After cooling to ambient temperatures, 60 mmol of olefin or allylic alcohol, an internal standard (cumene or pentadecane), and 9 ml of toluene (solvent) were added. For reactions with solid inorganic additive, 0.625 mmol solid was then added. The reaction was started by addition of 13.5 mmol TBHP. An exception to this procedure was the epoxidation of cyclohexenol, where only 20 mmol of cyclohexenol, 2 ml of toluene (solvent), 0.5 g activated zeolite 4 Å, decane as the internal standard, and 5 mmol TBHP were used.

Samples were analyzed by an HP 6890 gas chromatograph (cool on-column injection, HP-1 or HP-FFAP column).

Selectivity and yield were calculated as follows:

- selectivity of the epoxide related to the olefin converted

$$S_{\text{olefin}} = 100 \frac{[\text{epoxide}]}{[\text{reactant}]_0 - [\text{reactant}]} (\%); \quad [3]$$

- epoxide yield related to the peroxide

$$\text{yield} = 100\% \frac{[\text{epoxide}]}{[\text{TBHP}]_0}. \quad [4]$$

Note that the reactant:peroxide molar ratio was 4.4:1 (4:1 for cyclohexenol). The initial rate was defined as the epoxide formation in the first 5 min.

## 3. RESULTS

### Catalyst Synthesis

Prehydrolysis of MTMS before addition of the more reactive tetramethoxysilane was necessary to adjust the reactivity of the precursors for hydrolysis and condensation in the sol-gel process (8). The influence of prehydrolysis time was investigated for the 30Ae catalyst. The MTMS precursor was mixed with the acidic hydrolysant for 6, 12, or 24 h before addition of the other components of the sol-

TABLE 2

### Physico-Chemical characterization

Aerogel	$S_{\text{BET}}$ $\text{m}^2 \text{g}^{-1}$	$V_p^a$ $\text{cm}^3 \text{g}^{-1}$	$V_m^b$ $\text{cm}^3 \text{g}^{-1}$	$\langle d_p \rangle^c$ nm	$D_s^d$	$R^e$
0Ae	547	1.44	0.034	10.5 (60)	2.66	0.75
10Ae	446	1.41	0.014	12.2 (60)	2.62	0.57
20Ae	475	0.44	0.070	4.5 (22)	2.44	0.49
30Ae	505	0.54	0.087	4.8 (15)	2.52	0.56
30Ae-12h	447	0.54	0.085	5.8 (50)	2.42	0.57
30Ae-24h	420	0.47	0.060	4.6 (44)	2.41	0.53

<sup>a</sup> Designates the BJH cumulative desorption pore volume of pores in the maximum range 1.7–300 nm diameter.

<sup>b</sup> Micropore volume from *t*-method analysis; error 5–20%.

<sup>c</sup>  $\langle d_p \rangle = 4V_p/S_{\text{BET}}$ ; in parentheses the graphically assessed maximum of the pore size distribution, derived from the desorption branch, is given.

<sup>d</sup> Surface fractal dimension evaluated by fitting the fractal Frenkel-Halsey-Hill (FHH) isotherm in the range  $p/p_0 = 0.55$  to 0.88.

<sup>e</sup>  $R = S_{(\text{Si-O-Ti})}/S_{(\text{Si-O-Si})}$ , determined from FTIR spectra; estimated error  $\pm 10\%$ .

gel process (Table 1). The materials 30Ae, 30Ae-12h, and 30Ae-24 h were characterized by N<sub>2</sub> physisorption and IR spectroscopy (Table 2). The BET surface area as well as the pore volume decreased slightly with increasing prehydrolysis time. The average pore diameter for the differently prehydrolyzed materials showed no clear tendency, whereas the maximum of the pore size distribution was significantly shifted to larger pores for long prehydrolysis times. These findings point toward a denser network structure of the samples with longer prehydrolysis time, probably due to a more complete hydrolysis of the methylsilane precursor. IR transmission spectroscopy (see later) showed no significant differences in titania dispersion as a result of different prehydrolysis time (9).

The prehydrolysis test indicated that 6 h prehydrolysis is sufficient for obtaining a material with the desired properties (large pores, well-dispersed Ti in the silica matrix).

### Textural Properties—Nitrogen Physisorption

The textural properties gained from N<sub>2</sub> physisorption measurements are listed in Table 2. The BET surface areas were around  $500 \pm 50 \text{ m}^2 \text{g}^{-1}$ , indicating only a little dependence on the amount of organic modifier. The pore volume (in the pore size range 1.7–300 nm) decreased drastically by the organic modification. The mean pore diameter (assuming cylindrical pores) as well as the graphically assessed pore size maximum in the mesoporous range decreased as a result of the modification. A pronounced part of the micropore volume was observed for catalysts containing 20 and 30% methyl silicone. This significant fraction of micropore volume indicates a bimodal pore size distribution with a minor contribution of micropores.

The analysis of the fractal dimensions of the prepared aerogels gave values typical for aerogels (29). The surface

dimension  $D_S$  in the range 2.40–2.66 corroborates the strong fractal character of the aerogels.

### Thermal Stability of Aerogels

Calcination of the raw aerogel samples in air for removing organic residues is a crucial step prior to catalytic experiments. The calcination temperature had to be chosen very carefully to minimize the loss of methyl groups. A detailed investigation of the decomposition behavior of the raw aerogels in air was carried out using thermal analysis.

As an example, Fig. 1 depicts the calcination behavior of 30Ae in argon. The raw aerogel exhibited the most complex behavior because a large amount of organic residues was still present in the sample (Fig. 1a). The loss of mass was 39.4%, but did not completely originate from organic species, as a substantial desorption of water ( $m/z = 18$ ) from the hydrophilic material was observed.

A variety of mass signals attributed to C-containing species were noticed. For the raw sample (Fig. 1a), methanol (dominant  $m/z = 31$ ) and propanol (dominant  $m/z = 45$ ) were observed already at low temperatures (ca. 130°C). Acetylacetonate (dominant  $m/z = 43$ ) was detected at temperatures up to 500°C, with a maximum around 270°C. Apparently, acetylacetonate was still present after completion

of the sol-gel process and drying, which may be attributed to the high temperatures necessary to disintegrate titanium-acetylacetonate complexes (31). Overlapping signals for  $m/z = 27$ , 41, and 43 around 130°C might have originated from 2-propanol.

A large and broad signal of mass 15 was detected at elevated temperatures with a peak maximum at 600–610°C, which can be attributed to the decomposition of methyl silane groups. A very similar spectrum for the signal of  $m/z = 44$  due to the evolution of  $\text{CO}_2$  was also detected (not shown). The high temperatures required for the oxidation/degradation of methyl groups is in agreement with the known stability of the C–Si bond in methylsilanes (32).

The raw sample 30Ae was kept under vacuum for 24 h at 50°C. Figure 1b shows that this treatment was not sufficient for removing all organic impurities. A large peak of acetylacetonate was still observed, which could be removed only by calcination at 400°C (Fig. 1c).

Interestingly, the peak  $m/z = 18$  increased with the ongoing removal of organics. The relative amounts of water detected were 1 : 1.45 : 1.60 for the samples raw, treated in vacuum, and calcined, respectively. This observation indicates that the amount of water adsorbed by the sample during storage increased with decreasing content of organic residue. Thus, even the methyl-modified aerogels possessed

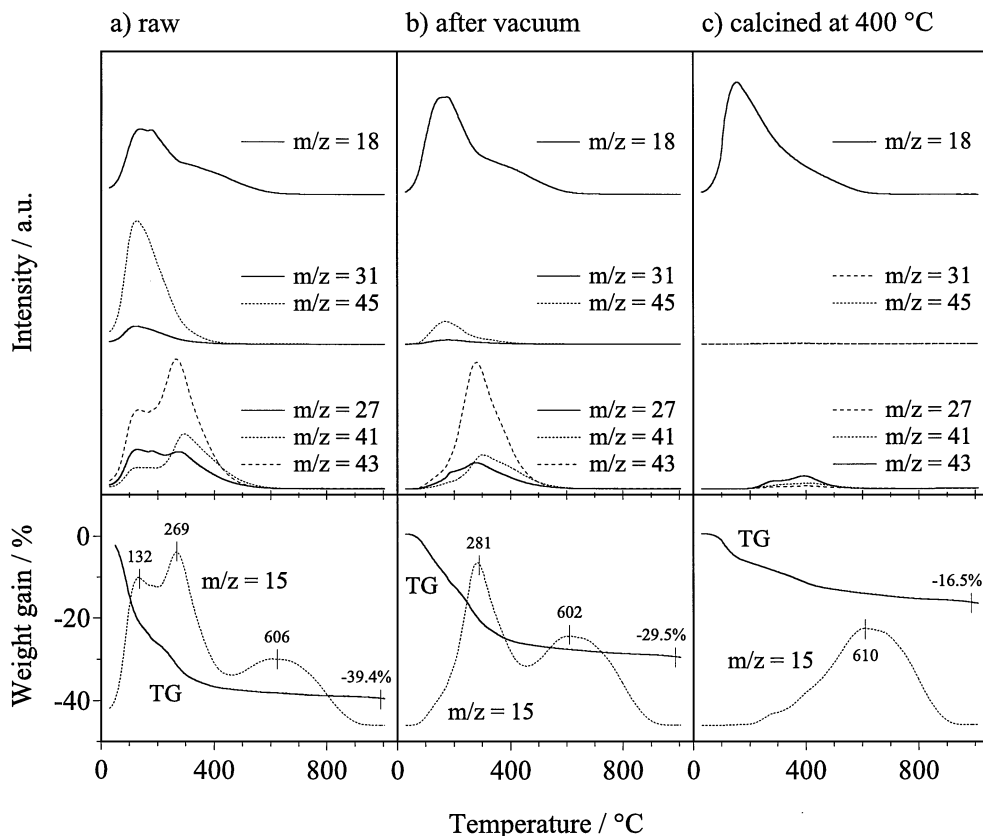


FIG. 1. Decomposition of 30Ae in air: (a) raw sample, (b) sample evacuated at 50°C in vacuum for 24 h, (c) sample calcined at 400°C.

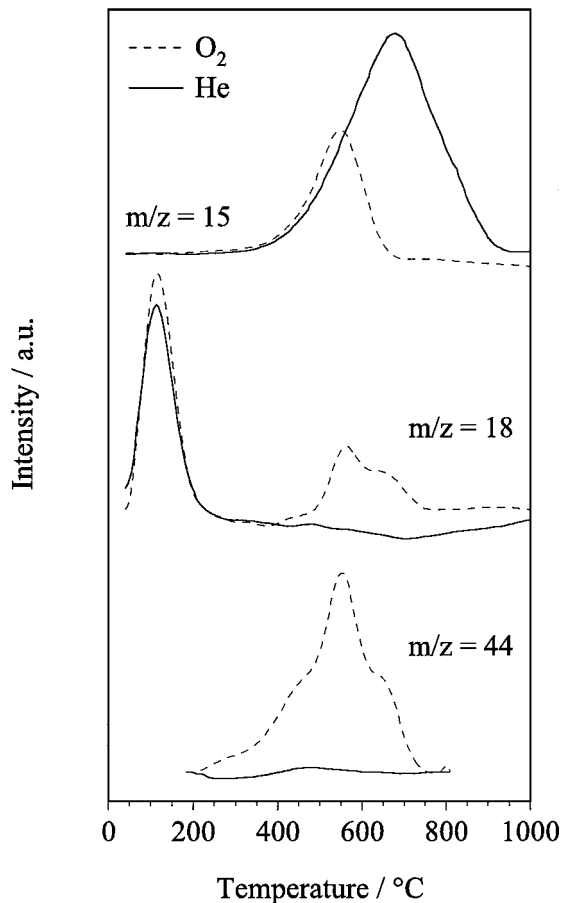


FIG. 2. Illustration of the quantification of the amount of methyl-modifier by means of thermogravimetry combined with mass spectroscopy; catalyst, 30Ae.

remarkable hydrophilicity. In order to minimize the detrimental effect of water on the epoxidation reaction, all catalysts were carefully redried *in situ* before use. In the following, only materials calcined at 400°C will be discussed.

The quantitative determination of the amount of methyl groups is illustrated in Fig. 2. The first run under He shows a dominant signal of  $m/z = 15$  ( $\text{CH}_3$  or fragments of alkanes) with only traces of  $m/z = 44$  ( $\text{CO}_2$ ). In the second run in oxygen with a new sample, the intensity of the  $\text{CO}_2$  signal corresponds to the difference in signal intensities of  $m/z = 15$  between the two runs due to the partial oxidation of  $\text{CH}_3$  groups. The loading of the catalyst with  $\text{CH}_3$  groups in  $\text{mg}(\text{CH}_3)/\text{g}(\text{catalyst})$  is depicted in Fig. 3. Comparison of the determined values with nominal loadings is difficult, since the exact composition of the catalysts is not known (especially the amount of silanol groups). The values, however, are in the expected range.

#### Ti Dispersion-FTIR Spectroscopy

The results of the FTIR studies are illustrated in Fig. 4. The upper part shows the spectrum from 500 to 4000  $\text{cm}^{-1}$ .

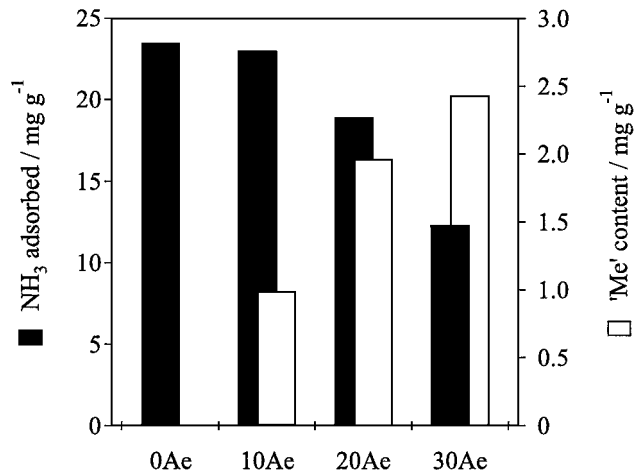


FIG. 3. Amount of adsorbed ammonia and methyl-content of the aerogels.

The region from 700–1500  $\text{cm}^{-1}$ , enlarged in the lower part, exhibits peaks assigned to different states of Si–O–Si and Si–O–Ti (33) connectivities, and peaks assigned to the Si–C vibration at ca. 1280  $\text{cm}^{-1}$  and to the C–H vibration at ca. 1400  $\text{cm}^{-1}$ . The upper part contains additional peaks at ca. 1625  $\text{cm}^{-1}$  assigned to water and a broad peak in the

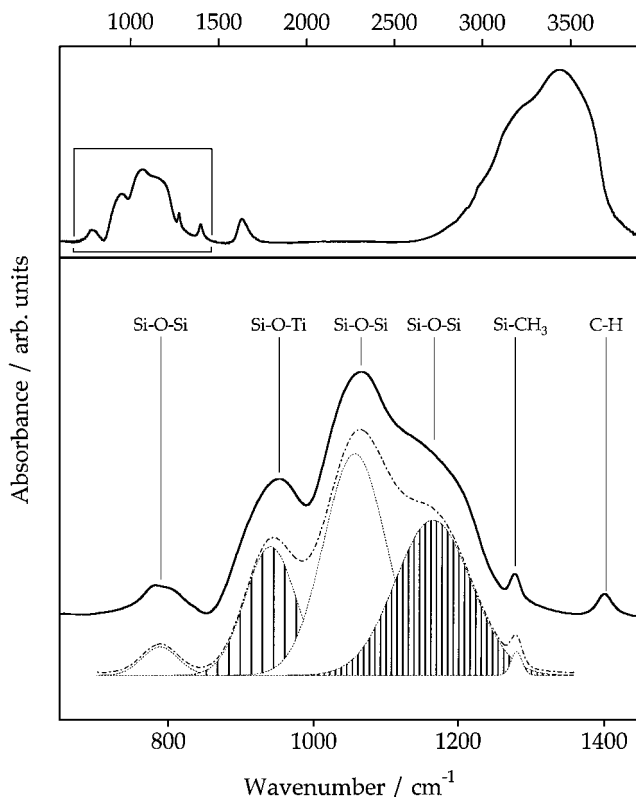


FIG. 4. FTIR spectrum of 30Ae (upper part) and deconvolution of the spectrum in the range 700–1400  $\text{cm}^{-1}$  (lower part).

range 2700–4000  $\text{cm}^{-1}$ , which results from vibrations of the O–H group, Si–O, and probably C–H bonds.

The ratio between the Si–O–Ti peak at 940–960  $\text{cm}^{-1}$  and the Si–O–Si peak around 1200  $\text{cm}^{-1}$  has previously been used as a means to quantify the dispersion of titania in the silica matrix. Although Brodsky *et al.* (34) noted that the Si–O–Ti peak is overlapped by a contribution from a Si–O<sup>-</sup> vibration, the estimation of the respective peaks ratio remains a suitable tool for the semi-quantitative determination of the Ti dispersion in the silica matrix. The values ( $R$ ) calculated from the deconvoluted peak areas using Eq. [1] are listed in Table 2. With the exception of 0Ae and 40Ae, with values around 0.75, all catalysts exhibited a ratio of ca. 0.55. Inclusion of methyl groups into the matrix diminished the titania dispersion to a certain degree. This effect could be a consequence of the reduced reactivity of the methyl-containing silane precursor in the sol-gel process leading to an enhanced homonuclear reaction of the Ti precursors. Note also that the degree of Ti dispersion of 0.49–0.57 was still very high compared to other titania–silica aerogels prepared by different sets of sol-gel parameters (9).

#### Ammonia Adsorption–DRIFT Spectroscopy and Thermal Analysis

The ability of the aerogels to adsorb ammonia was investigated by DRIFT spectroscopy measurements; the spectra are presented in Fig. 5. In the left part, the difference spectra (spectrum of unloaded sample subtracted from spectrum with adsorbed ammonia) of the modified catalysts are

shown. The vibrational bands are attributed to the presence of Brønsted (**B**) or Lewis (**L**) sites (35). Both types of acidic sites are present on the aerogel surface, independent of the composition. Interesting is the strongly negative peak at ca. 2950  $\text{cm}^{-1}$  for modified catalysts, which is attributed to the C–H stretch vibration (36). Since DRIFT spectroscopy is a surface sensitive method, these measurements show that the methyl groups are (at least partially) located at the surface and accessible for ammonia, and the amount of these groups increases with increasing nominal methyl-content.

The right part illustrates the desorption behavior of ammonia. The disappearance of the negative O–H peaks at ca. 3700  $\text{cm}^{-1}$  and the negative C–H at 2950  $\text{cm}^{-1}$  is well visible at higher temperatures. This indicates that at 50°C both –OH and –CH<sub>3</sub> groups are covered by (weakly and strongly adsorbed) ammonia.

The acidity of the catalysts was also investigated by means of pulse thermal analysis (PTA, (26)). The quantitative determination of strongly adsorbed (chemisorbed) ammonia is facilitated by following the mass change of the sample upon the introduction of small ammonia pulses.

The amount of chemisorbed ammonia as a function of catalyst composition is illustrated in Fig. 3. With an increasing amount of methyl groups the ability of the calcined materials to adsorb NH<sub>3</sub> decreased. The unmodified material adsorbed twice the amount as catalyst 30Ae. The remaining adsorption for the latter is attributed mainly to the presence of residual silanol groups and Ti sites. The small differences in the catalyst surface areas had relatively little effect on ammonia adsorption (Table 2).

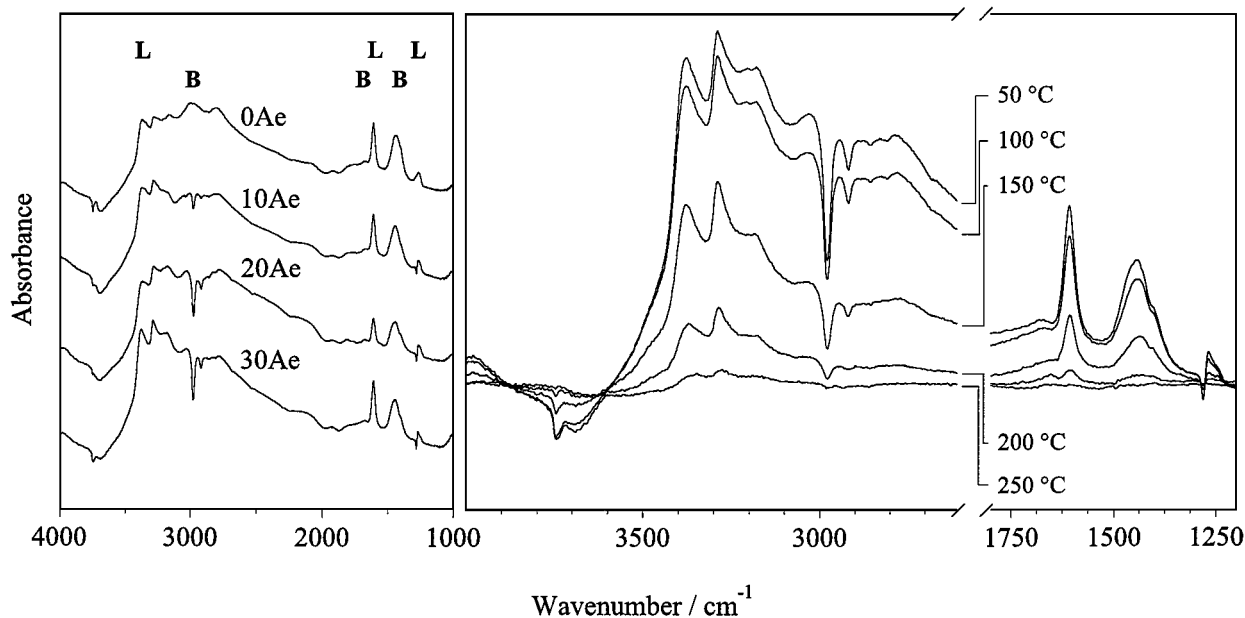


FIG. 5. DRIFT spectra of the aerogels. (Left) Difference spectra of catalysts treated with ammonia at 50°C (**B**, Brønsted sites; **L**, Lewis sites). (Right) Difference spectra of the catalyst 30Ae during heating from 50 to 250°C after ammonia adsorption.

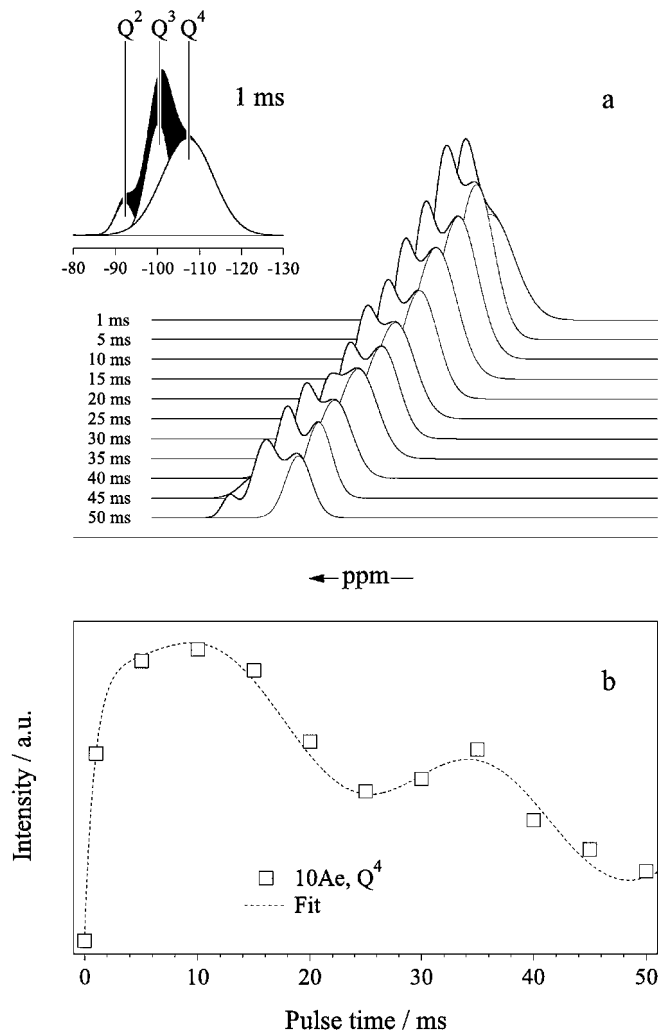


FIG. 6. Illustration of the NMR analysis for the 10Ae catalyst. (a)  $^{29}\text{Si}$  CP/MAS-signal as a function of pulse time (inset: deconvolution of the signal in the range  $-80$  to  $130$  ppm); (b) Fit of the theoretical function to the experimental intensities for the  $\text{Q}^4$  site of 10Ae.

### Bulk Structure-NMR Characterization

NMR examination of the aerogel structure was based on the variation of the pulse time for  $^{29}\text{Si}$ -CP-MAS experiments (30). An example of the analysis procedure is presented in Fig. 6 for the catalyst 10Ae. The inset in the upper part (a) shows the deconvolution of the signal in the range  $-85$  to  $-130$  ppm. The peaks are assigned to the  $\text{Q}^2$  (ca.  $-92$  ppm),  $\text{Q}^3$  (ca.  $-100$  ppm), and  $\text{Q}^4$  sites (ca.  $-109$  ppm). Theoretically, also the  $\text{T}^2$  (ca.  $-56$  ppm) and the  $\text{T}^3$  species (ca.  $-64$  ppm) should have been observed but they were not discernible probably due to their low concentration. Deconvolution is illustrated in Fig. 6a for the different pulse times. The intensities of the  $\text{Q}^4$  sites were fitted according to Eq. [2] as shown in Fig. 6b. The calculated parameters are listed in Table 3. Comparison with

previous publications (30, 37–40) shows that the values are similar to those obtained for titania-silica xerogels.

The most interesting parameters are the intensity of the respective species ( $M_0$ ), the cross polarization time ( $T_{\text{SiH}}$ ), and the parameter  $a$  that expresses the fraction of the S-spins for which the spin-temperature concept is valid. The spin-diffusion time  $T_{\text{HH}}$  and the relaxation time  $T_{1\rho}$  were infinite or large in almost all experiments and thus gave no clues about significant differences for the various materials. The oscillation frequency  $b$  varied in a relatively wide range and thus points to complex geometries involved in the oscillatory magnetization transfer process (30).

Parameter  $a$  changed from lower values for 0Ae (mean value around 0.4) to higher values for modified catalysts (mean values around 0.79 for 10Ae, 0.82 for 20Ae, and 0.84 for 30Ae). This result suggests that for the unmodified catalyst, less protons were available for the application of the spin-temperature concept; i.e., the network was more cross-linked. This difference was additionally evidenced by the increased contribution of  $\text{Q}^4$  sites.

The  $T_{\text{SiH}}$  values increased within one series (T or Q sites). This enhancement is explained by the vicinity of OH protons for the  $\text{T}^2$ ,  $\text{Q}^2$ , and  $\text{Q}^3$  sites. With an increasing distance between the Si atom and the proton reservoir, the cross-polarization rate,  $1/T_{\text{SiH}}$ , decreased.

The distribution of Q sites in the unmodified 0Ae aerogel reflects a strongly cross-linked silica matrix. The amount of OH group carrying Si atoms (45.2% of the total amount of Si) is, however, still large enough to explain the typical light structure and hydrophilicity (acidity) of titania-silica aerogels. As a measure of cross-linkage, the values of the relative intensities of  $\text{Q}^4$  and  $\text{Q}^3$  sites were compared. The corresponding ratio for the 0Ae material was  $\text{Q}^3:\text{Q}^4 = 1:1.3$  (see Table 3). The incorporation of an increasing amount of methyl groups into the matrix shifted this ratio up to 1:2.3 for 30Ae. This shift could either be explained by a stronger cross-linkage (relatively more  $\text{Q}^4$  sites) or by a substitution of OH groups by  $\text{CH}_3$  groups (relatively less  $\text{Q}^3$  sites). On the basis of the conclusions for the parameter  $a$ , and the DRIFT and PTA measurements discussed above, we propose that the substitution of  $-\text{OH}$  groups by methyl groups is dominant.

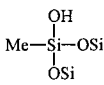
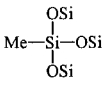
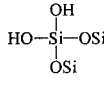
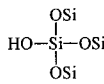
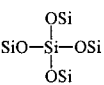
The amount of T sites related to the total Si content supports the preparation and calcination procedure and confirms the quantitative determination by TA analysis for the 20Ae and 30Ae catalysts.

### Surface Composition-XPS

Quantitative analysis of the composition in the surface layer (Table 4) was based on the integration of C 1s, O 1s, Ti 2p, and Si 2p peaks using known sensitivity factors (41). The dominant atom found with ca. 68 at.% was oxygen. The surface atomic ratio of Ti and Si was  $0.21 \pm 0.1$ , barely above the bulk atomic ratio of 0.19. Earlier, a significant surface



**TABLE 3**  
Parameters Characterizing the  $^{29}\text{Si}$  NMR Spectra of the Aerogels<sup>a</sup>

Aerogel	Structural type	$M_Q/\%$	ratios <sup>b</sup>	$T_{\text{SiH}}/\text{ms}$	$T_{\text{HH}}/\text{ms}$	$T_{1\rho\text{H}}/\text{ms}$	$a$	$b/\text{rad ms}^{-1}$	Types
0Ae	$Q^2$	2.8±0.4	-	(1)	(∞)	(∞)	(0.5)	0.70±0.04	
	$Q^3$	42.4±2.8	1	1.69±0.98	(∞)	(∞)	0.58±0.08	0.28±0.02	
	$Q^4$	54.8±4.1	1.3	2.19±7.72	26.0±20.7	(∞)	0.23±0.67	0.56±0.03	
10Ae	$T^2$	not discernible							$T^2$ : 
	$T^3$	not discernible							
	$Q^2$	3.8±0.7	-	0.16±0.16	(∞)	58.2±24.4	(0.78)	0.77±0.06	
	$Q^3$	40.0±3.5	1	(0.5)	(∞)	50.1±8.8	(0.8)	0.70±0.03	
	$Q^4$	56.2±0.03	1.4	0.94±0.15	(∞)	48.7±4.5	0.79±0.07	0.53±0.01	$T^3$ : 
20Ae	$T^2$	6.8±1.0	1	(0.90)	100±156	(∞)	0.22±0.37	0.68±0.03	
	$T^3$	12.9±1.2	1.9	1.24±0.80	(∞)	(∞)	0.78±0.14	0.51±0.05	
	$Q^2$	3.7±0.4	-	2.24±1.63	(∞)	(∞)	0.82±0.17	0.50±0.08	$Q^2$ : 
	$Q^3$	29.0±1.4	1	(2.40)	(∞)	(∞)	(0.85)	0.55±0.05	
	$Q^4$	47.6±2.7	1.6	2.62±0.91	(∞)	(∞)	0.85±0.10	0.45±0.04	
30Ae	$T^2$	10.3±1.7	1	1.70±1.45	(∞)	142±131	0.78±0.18	0.57±0.05	$Q^3$ : 
	$T^3$	15.3±2.7	1.5	2.76±1.56	77.8±67.9	160±176	0.86±0.31	1.17±0.11	
	$Q^2$	3.0±0.4	-	1.43±1.30	(∞)	(∞)	0.76±0.21	0.94±0.06	
	$Q^3$	21.7±0.8	1	2.21±0.52	(∞)	(∞)	(0.80)	0.77±0.02	$Q^4$ : 
	$Q^4$	49.7±2.8	2.3	2.51±0.70	(∞)	(∞)	(0.98)	0.99±0.34	

<sup>a</sup> Values in brackets were kept constant during the fitting procedure.

<sup>b</sup> Ratios of  $T^3$  to  $T^2$ , and  $Q^4$  to  $Q^3$ , respectively.

enrichment of Si was observed for 2–20 wt%  $\text{TiO}_2$ - $\text{SiO}_2$  aerogels (42). The almost identical surface and bulk Ti concentration in this work may be explained by the different preparation conditions.

### Morphology—HRTEM

The high resolution electron micrograph of the 0Ae catalyst is shown in Fig. 7. The unmodified material exhibits

**TABLE 4**  
XPS Analysis

Aerogel	Composition [at%]				
	C 1s	O 1s	Ti	Si 2p	Ti/Si <sup>a</sup>
0Ae	7.2	67.9	4.0	20.9	0.22
10Ae	5.7	68.4	4.4	21.5	0.20
20Ae	6.3	68.5	4.5	20.7	0.22
30Ae	12.4	63.9	4.2	19.6	0.21

<sup>a</sup> Ti/Si atomic ratio at the surface (nominal value 0.19).

the typical amorphous aerogel structure (8). A few crystalline particles below 1 nm could be perceived, which are attributed to titania nanoparticles, the presence of which has been confirmed earlier (4, 9). Note that all aerogels were X-ray amorphous.

Although the 30Ae catalyst (not shown) contained a large fraction of modified silicon sites, no significant differences could be observed compared to the unmodified material. No crystallinity was detected either by HRTEM or by powder X-ray diffraction. Electron dispersive X-ray analysis of different regions in both catalysts indicated a ratio Ti : Si of 0.18, in good agreement with the nominal value (0.19).

### Catalytic Experiments

*Addition of neutral and basic inorganic compounds.* The influence of inorganic additives on the epoxidation of cyclohexene with TBHP at 60°C over a 30Ae catalyst is depicted in Fig. 8. For the sake of better comparability, the cation was always sodium. Over the range from NaCl to

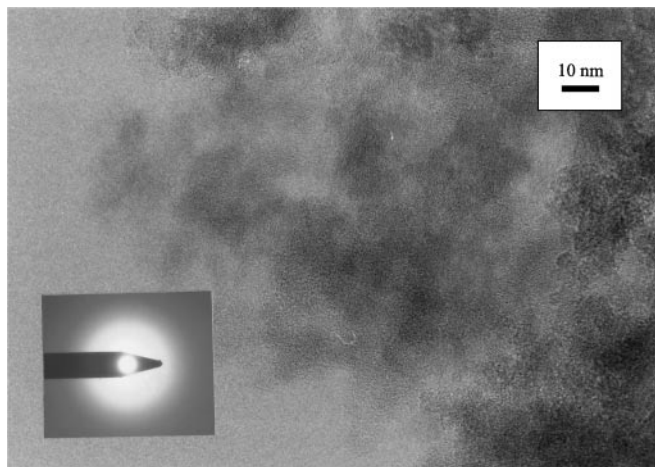


FIG. 7. High-resolution electron micrograph of pure titania-silica aerogel 0Ae.

NaOH, maxima in both the initial epoxide formation rate and the yield after 90 min were observed. The initial rate did not follow the same pattern as the yield, being highest for NaOAc instead of  $\text{NaHCO}_3$ . Selectivity to the epoxide related to the olefin converted was high for all reactions; no other products beside the epoxide were observed by GC analysis.

**Influence of surface methyl groups.** The catalytic behavior of the aerogels was investigated in the epoxidation of various olefins and allylic alcohols. The size and polarity of these substrates, and the electron density at the C=C bond,

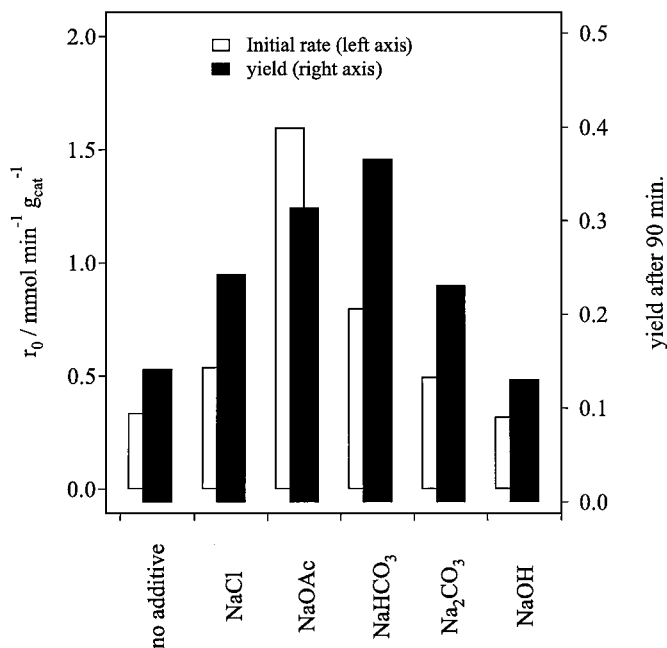


FIG. 8. Influence of neutral and basic additives on the epoxidation of cyclohexene with TBHP over a 30Ae catalyst (60 mmol cyclohexene, 13.4 mmol TBHP, 9 ml toluene, 0.625 mmol additive,  $60^\circ\text{C}$ ).

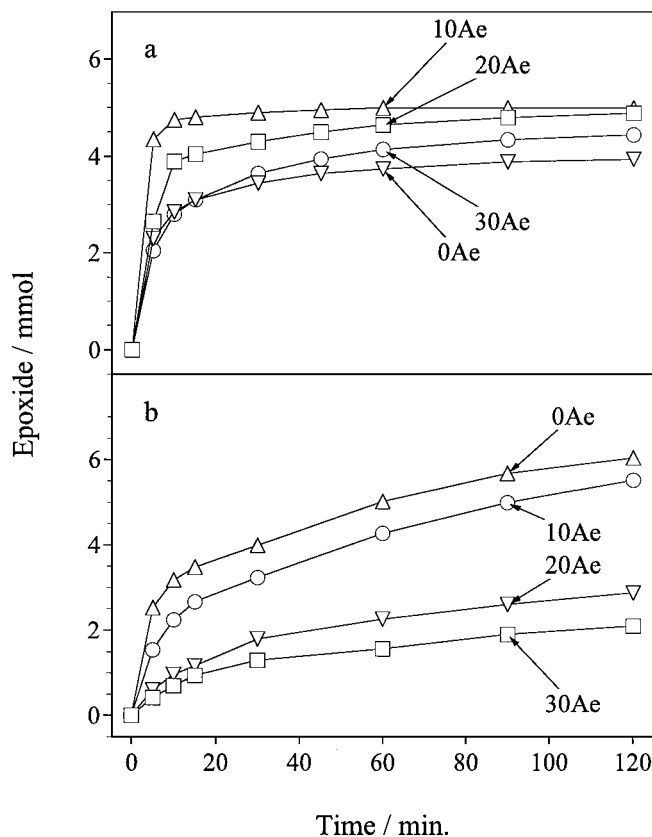


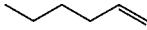

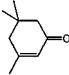
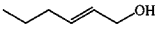
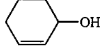
FIG. 9. Influence of methyl modification on the reaction of (a) cyclohexenol and (b) cyclohexene with TBHP (for conditions, see Experimental).

were varied. The time-resolved formation of epoxides is illustrated in Fig. 9 for the examples of cyclohexene and cyclohexenol oxidation. These kinetic curves can be well characterized by the initial rate (epoxide formation in 5 min,  $r_0$ ) and the amount of epoxide produced in a longer time period (2–5 h). The latter value provides information on possible catalyst deactivation. Besides  $r_0$  and epoxide yields, Table 5 lists also the epoxide selectivities at 30–100% conversion.

There is a general negative effect of surface methyl groups on the epoxide formation in the oxidation of 1-hexene, cyclohexene, and isophorone. The detrimental influence of organic modification of titania-silica is more pronounced for bulky cyclic olefins. The moderate reactivity of isophorone, as compared to cyclohexene, is due to the electron deficiency of the C=C double bond ( $\alpha$ -carbonyl group, (5)). All four catalysts were highly selective in these three reactions and no other product beside the epoxides could be detected by GC analysis. This behavior is typical for well designed titania-silica aerogels and for reactions carried out under dry conditions (4–6).

The opposite effect of surface modification was observed in the oxidation of allylic alcohols. In this type of epoxidations the performance of titania-silica is moderate (10). The epoxide selectivity is usually diminished by

TABLE 5  
Epoxidation Reactions with Unmodified and Methyl-Modified Catalysts

Reactant	Temperature [°C]	characteristic values <sup>a</sup>	Catalyst			
			0Ae	10Ae	20Ae	30Ae
	60	$r_0$ / mmol g <sup>-1</sup> min <sup>-1</sup>	0.11	0.07	0.13	0.11
		epoxide after 2 h / mmol	1.47	1.21	1.23	1.09
	60	$r_0$ / mmol g <sup>-1</sup> min <sup>-1</sup>	2.02	1.23	0.49	0.34
		epoxide after 2 h / mmol	6.03	5.49	2.81	2.14
	60	$r_0$ / mmol g <sup>-1</sup> min <sup>-1</sup>	0.40	0.36	0.34	0.28
		epoxide after 2 h / mmol	1.33	0.84	0.62	0.52
	60	$r_0$ / mmol g <sup>-1</sup> min <sup>-1</sup>	0.68	0.66	0.47	0.84
		epoxide after 5 h / mmol	3.02	2.95	3.48	4.02
		selectivity at 30% conv. <sup>b</sup>	56%	72%	89%	79%
	90	$r_0$ / mmol g <sup>-1</sup> min <sup>-1</sup>	6.57	12.4	7.57	5.86
		epoxide after 10 min / mmol	2.85	4.75	3.90	2.80
		selectivity at 90% conv. <sup>b</sup>	73%	98%	82%	78%
		selectivity at 100% conv. <sup>b</sup>	70%	94%	82%	76%

<sup>a</sup>  $r_0$ , amount of epoxide formed during initial 5 min; other definitions see text.

<sup>b</sup> Conversion of the allylic alcohol is related to the initial amount of peroxide.

acid-catalyzed side reactions (dimerization, oligomerization, isomerization, and epoxide ring opening) and by oxidation of the alcoholic OH group. The positive effect of surface methyl groups was more pronounced in the oxidation of cyclohexenol than for the linear trans-2-hexenol. 10Ae afforded almost double the initial rate, compared to 0Ae, and very high epoxide selectivity (94–98%) at 90–100% peroxide conversion after about 10 min (Table 5). To our knowledge, these are the highest values reported to date for the solid-catalyzed epoxidation of cycloalkenols; only TS-1 affords similar high yields in the epoxidation of linear alkenols ((43) and references therein).

#### 4. DISCUSSION

##### Characterization of Organically Modified Titania–Silica Aerogels

Modification of the surface of titania–silica aerogels by covalently bound methyl groups can simply be accomplished by the partial replacement of the Si precursor tetramethoxysilane by methyltrimethoxysilane (11, 12). However, the considerably lower sol-gel activity of the latter compound required a redesign of our former synthesis route (9). On the basis of preliminary experiments, several

important parameters have been altered, including the Ti precursor, the prehydrolysis procedure, and the hydrolysis level. Accordingly, the characterization of the new catalyst series 0Ae–30Ae aimed at confirming some structural features crucial for good epoxidation performance, such as high surface area, mesoporous structure, and high abundance of Ti–O–Si linkages, as well as presence of methyl groups covalently bound to the silica matrix.

The mesoporosity of all materials tested was not only confirmed by N<sub>2</sub> physisorption, but also by the catalytic activity in the oxidation of bulky substrates. Microporous catalysts are not suitable for the epoxidation of such molecules. The introduction of higher amounts of methyl groups (20Ae, 30Ae) lowered the mean pore diameter, whereas the surface area was barely influenced by the composition. Similarly, the practically constant surface Ti/Si atomic ratio close to the designed bulk ratio suggests that the different sol-gel reactivity of the precursors was sufficiently well compensated. According to IR investigations, Ti dispersion within the silica matrix seems to be slightly reduced by the insertion of methyl groups. Interestingly, small crystalline domains were only discernible for the unmodified catalyst in the TEM micrographs; all aerogels were X-ray amorphous.

The incorporation of covalently bound methyl groups into the silica matrix was confirmed by various methods.

Thermoanalysis revealed significant Si-C bond breaking only at elevated temperatures (400–900°C). Such high thermal stability can only be explained by relatively stable, covalent bonds. The IR spectra showed bands which are attributed to Si-C and C-H bonds. The NMR measurements evidenced T sites (T<sup>2</sup> and T<sup>3</sup>) that can only be explained by a covalent methyl modification. The relative amounts of Si-C sites correspond well with the nominal (designed) contents of the aerogels.

The DRIFT spectra gave clear evidence for the presence of methyl groups at the surface. The peaks in the region of the C-H bond vibrations (ca. 3000 cm<sup>-1</sup>) are the result of the coverage of the modified surface by ammonia. Less ammonia is adsorbed on modified catalysts, which points to a partial modification of the surface. Distribution of the methyl groups over the surface can be estimated by NMR measurements. The particular Si species bore a well-defined amount of terminal groups like OH and CH<sub>3</sub>. Only OH groups were detected on the surface of the unmodified aerogel. On the basis of the data presented in Table 3, the fraction of methyl groups compared to the total amount of surface groups (CH<sub>3</sub> and OH) is estimated to be 15–40% for the catalysts 0Ae–30Ae.

In summary, the preparation procedure yielded well-dispersed titania-silica mixed oxides with a varying amount of Si-CH<sub>3</sub> groups on the catalyst surface. Organic modification led to a partial exchange of surface silanol groups with methyl groups. Analysis of the physico-chemical properties showed that the major difference among the investigated materials can be attributed to the modification by methyl groups.

#### *Catalytic Performance of the Aerogels*

The epoxidation activity of titania-silica is attributed to the Lewis acidity of Ti-(OSi)<sub>4</sub> sites (1). It has been shown (5, 44) that the Ti-peroxo complex is markedly more acidic than the Ti-(OSi)<sub>4</sub> structural unit and rather active, e.g., in epoxide ring opening reactions. Another reason for acid-catalyzed side reactions during epoxidation is the presence of surface Si-OH groups (Brønsted sites).

Ammonia adsorption measurements by DRIFT spectroscopy confirmed the presence of both Lewis and Brønsted acidic sites on all four aerogels. Pulse thermal analysis indicated that the amount of NH<sub>3</sub> decreased significantly with increasing degree of organic modification of the aerogels. This may be explained by the successive replacement of surface Si-OH groups by Si-CH<sub>3</sub> groups. The decreased hydrophilicity of methyl-modified titania-silica has been confirmed by Maier and co-workers (12) and Figueras and co-workers (11).

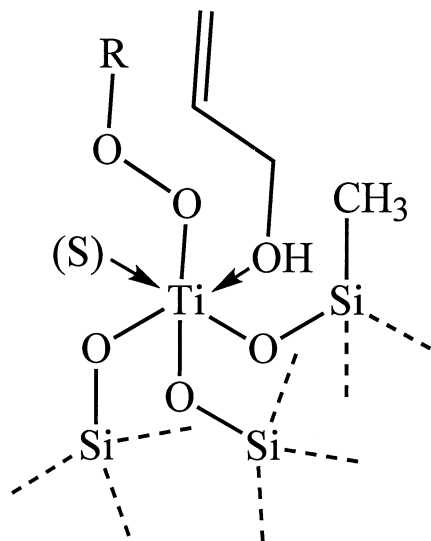
A striking positive effect of weakly basic inorganic salts was observed in the epoxidation of cyclohexene over 30Ae (Fig. 8). The initial rate and the epoxide yield after 90 min increased by a factor of up to 3–4 in the presence of NaOAc

and NaHCO<sub>3</sub>. The minor solubility of inorganic salts in the weakly polar reaction medium has been confirmed earlier (43). In this reaction, the epoxide selectivity was very high: by-product formation was not detectable by GC analysis even after 2 h. Polymerization-type side reactions, resulting in large nonvolatile products which could block some active sites in the pores are also not likely, as the intermediate dimers and trimers are sufficiently volatile for GC detection. Accordingly, the most probable explanation for the rate acceleration is the interaction of the inorganic additives with the Ti active sites. This interaction changes the stability (and thus the reactivity) of the Ti-peroxo complex ((2) and references therein) leading to a volcano-type relationship. Note that this is the first case that the effect of basic or neutral salts could be localized to their interaction with the Ti-peroxo complex in titania-silica and any influence on acid- or base-catalyzed side reactions could be excluded.

The influence of surface methyl groups on the catalytic performance of titania-silica aerogels was investigated in the epoxidation of five different reactants (Table 5). No positive effect of methyl-modification was observed in the epoxidation of 1-hexene, cyclohexene, and isophorone. The high selectivity of unmodified aerogel (0Ae) was preserved, but in the latter two reactions (cyclohexene, isophorone) the rate of epoxide formation was diminished markedly over the organically modified aerogels. This behavior might be attributed to the slightly lower surface area, the lower Ti dispersion in the silica matrix, and the increased microporosity of modified aerogels. Probably the most important influence of surface methyl groups is the reduced hydrophilicity of the aerogels (11, 45, 46). The crucial role of surface polarity in the adsorption of organic reaction components is demonstrated by the recently reported strong solvent effect (11): the rate of cyclohexene epoxidation increased or decreased by methyl modification of titania-silica in *tert*-butanol and acetonitrile, respectively.

A strong positive effect of methyl-modification was observed in the epoxidation of linear and cyclic alcohols (Table 5). Not only the rate of epoxide formation but also the epoxide selectivities are markedly better for the modified aerogels. The higher epoxide selectivities are partially due to the suppressed acidity of modified aerogels, as shown by ammonia adsorption (Fig. 3). However, the enhanced rate of epoxide formation alone can explain the higher selectivity, even if the rate of acid-catalyzed side reactions remained constant (e.g., 10Ae, cyclohexenol oxidation, Table 5).

Another feasible explanation for the observed positive effect in allylic alcohol epoxidation is the strong interaction of alkenols with the Ti active site, as illustrated in Scheme 1 (2). It is assumed that during epoxidation of the C=C bond by one of the peroxo O atoms, the OH group of the allylic alcohol is interacting with Ti. Note that the additional coordination of a polar (solvent) molecule is also possible,



(S) = Solvent

SCHEME 1

leading to the favored sixfold coordination and octahedral structure (31, 47, 48). In this position the reactant can easily interact with the neighboring surface atoms. Substitution of some neighboring surface  $-OH$  groups by  $-CH_3$  groups may have a significant effect on the stability/reactivity of allylic alcohols anchored to Ti. On the contrary, this effect is missing in the epoxidation of simple olefins, where the (nonanchored) reactant may be relatively far from the surface methyl groups. Further support for this assumption will be supplied by the study of other types of organically modified aerogels (49).

## 5. CONCLUSIONS

Careful selection of the sol-gel parameters resulted in a series of organically modified 20 wt% titania–80 wt% silica aerogels with similar physico-chemical characteristics, except the presence of a varying amount of covalently bound surface methyl groups. All four aerogels are predominantly mesoporous with high abundance of Ti–O–Si connectivity and high surface area (around  $500 \text{ m}^2 \text{ g}^{-1}$ ). The almost constant surface Ti/Si atomic ratio demonstrates that the different reactivity of Ti and Si precursors was successfully compensated in the sol-gel synthesis.

$^{29}\text{Si}$  CP/MAS NMR and pulse thermal analysis provided new insights into the characteristic features of organically modified aerogels (methyl groups covalently bound to the silica network, partial substitution of surface  $-OH$  groups by  $-CH_3$  groups, degree of cross-linkage in bulk structure).

The unprecedented high activity and selectivity of the methyl-modified aerogel 10Ae in the epoxidation of cyclohexenol with TBHP may be attributed to the special interactions between the reactant anchored to the Ti site and the neighboring surface  $-OH$  and  $-CH_3$  groups. The performance of this catalyst is promising for a future practical application: 90% conversion was achieved in about 10 min, and the selectivity to epoxide was 98% in this demanding reaction.

## ACKNOWLEDGMENTS

Thanks are due to Dr. Jan-Dierk Grunwaldt for XPS measurements and Marco Dusi for performing 1-hexenol epoxidation. We also thank Dr. Frank Krumeich for the TEM and EDX measurements. Financial support of our work provided by the ETH-Jubiläumsfond (TEMA- project) is gratefully acknowledged.

## REFERENCES

- Sheldon, R. A., *J. Mol. Catal.* **7**, 107 (1980).
- Notari, B., *Adv. Catal.* **41**, 253 (1996).
- Wulff, H. P., Patent, 1975, Shell Oil Company, USA.
- Hutter, R., Mallat, T., and Baiker, A., *J. Catal.* **153**, 177 (1995).
- Hutter, R., Mallat, T., and Baiker, A., *J. Catal.* **157**, 665 (1995).
- Hutter, R., Mallat, T., Peterhans, A., and Baiker, A., *J. Mol. Catal. A: Chemical* **138**, 241 (1999).
- Hutter, R., Mallat, T., Dutoit, D., and Baiker, A., *Top. Catal.* **3**, 421 (1996).
- Brinker, C. J., and Scherer, G. W., "Sol-Gel Science." Academic Press, Boston, 1990.
- Dutoit, D. C. M., Schneider, M., and Baiker, A., *J. Catal.* **153**, 165 (1995).
- Dusi, M., Mallat, T., and Baiker, A., *J. Mol. Catal. A: Chemical* **138**, 15 (1999).
- Kochkar, H., and Figueras, F., *J. Catal.* **171**, 420 (1997).
- Klein, S., and Maier, W. F., *Angew. Chem.* **108**, 2376 (1996).
- Chiari, M., Nesi, M., and Righetti, P. G., in "Surface Modification of Silica Walls: A Review of Different Methodologies," p. 1. CRC Press, Boca Raton, 1996.
- Clark, J. H., and Macquarrie, D. J., *J. Chem. Soc., Chem. Commun.* 853 (1998).
- Gründling, C., Eder-Mirth, G., and Lercher, J. A., *J. Catal.* **160**, 299 (1996).
- Kim, J.-H., Okajima, M., and Niwa, M., *Stud. Surf. Sci. Catal.* **105**, 1965 (1997).
- Slavov, S. V., Chuang, K. T., and Sanger, A. R., *J. Phys. Chem.* **100**, 1628 (1996).
- Vansant, E. F., Voort, P. V. D., and Vrancken, K. C., *Stud. Surf. Sci. Catal.* **93**, 1 (1995).
- Yokogawa, H., and Yokoyama, M., *J. Non-Cryst. Sol.* **186**, 23 (1995).
- Bhatia, S. K., Shriver-Lake, L. C., Prior, K. J., Georger, J. H., Calvert, J. M., Bredehorst, R., and Ligler, F. S., *Anal. Biochem.* **178**, 408 (1989).
- Grobe, J., *Organosil. Chem. II* 591 (1994).
- Jönsson, U., Malmqvist, M., Olofsson, G., and Rönnerberg, I., *Methods Enzymol.* **137**, 381 (1988).
- Khatib, I. S., and Parish, R. V., *J. Organometal. Chem.* **369**, 9 (1989).
- Vandenberg, E., Elwing, H., Askendal, A., and Lundström, I., *J. Colloid Interface Sci.* **143**, 327 (1991).
- Maciejewski, M., Müller, C. A., Mallat, T., and Baiker, A., in preparation.
- Maciejewski, M., Müller, C. A., Tschan, R., Emmerich, W. D., and Baiker, A., *Thermochim. Acta* **295**, 167 (1997).

27. Maciejewski, M., and Baiker, A., *Thermochim. Acta* **295**, 95 (1997).
28. Broekoff, J. C. P., in "Preparation of Heterogeneous Catalysts II," p. 663. Elsevier, Amsterdam, 1979.
29. Jarzebski, A. B., Lorenc, J., Aristov, Y. I., and Lisitza, N., *J. Non-Cryst. Sol.* **190**, 198 (1995).
30. Walther, K. L., Wokaun, A., and Baiker, A., *Mol. Phys.* **71**, 769 (1990).
31. Clark, R. J. H., in "The Chemistry of Titanium and Vanadium," p. 1. Elsevier, Amsterdam, 1968.
32. Witte, B. M. D., Commers, D., and Uytterhoeven, J. B., *J. Non-Cryst. Sol.* **202**, 35 (1996).
33. Schraml-Marth, M., Walther, K. L., Wokaun, A., Handy, B. E., and Baiker, A., *J. Non-Cryst. Sol.* **143**, 93 (1992).
34. Brodsky, C. J., and Ko, E. I., *J. Mater. Chem.* **4**, 651 (1994).
35. Liu, Z., Tabora, J., and Davis, R. J., *J. Catal.* **149**, 117 (1994).
36. Atkins, P. W., "Physical Chemistry," Oxford University Press, Oxford, 1990.
37. Handy, B. E., Baiker, A., Walther, K. L., and Wokaun, A., in "Synthesis and Properties of New Catalysts: Utilization of Novel Materials Components and Synthetic Techniques," p. 107. Mat. Res. Soc., 1990.
38. Walther, K. L., Wokaun, A., Handy, B. E., and Baiker, A., *J. Non-Cryst. Sol.* **134**, 47 (1991).
39. Handy, B., Walther, K. L., Wokaun, A., and Baiker, A., *Stud. Surf. Sci. Catal.* **63**, 239 (1991).
40. Schraml-Marth, M., Walther, K. L., Wokaun, A., Handy, B. E., and Baiker, A., *J. Non-Cryst. Sol.* **143**, 93 (1992).
41. Wagner, C. D., Davis, L. E., Zeller, M. V., Teller, J. A., Raymond, R. M., and Gede, L. H., *Surf. Interface Anal.* **3**, 211 (1981).
42. Dutoit, D. C. M., Göbel, U., Schneider, M., and Baiker, A., *J. Catal.* **164**, 433 (1996).
43. Dusi, M., Mallat, T., and Baiker, A., *J. Catal.* **173**, 423 (1998).
44. Davis, R. J., and Liu, Z., *Chem. Mater.* **9**, 2311 (1997).
45. Lee, K.-H., Kim, S.-Y., and Yoo, K.-P., *J. Non-Cryst. Sol.* **186**, 18 (1995).
46. Klein, S., Thorimbert, S., and Maier, W. F., *J. Catal.* **163**, 476 (1996).
47. McAuliffe, C. A., and Bricklebank, N., in "Titanium: Inorganic & Coordination Chemistry," p. 4197. Wiley, Chichester, 1994.
48. Mintz, E. A., in "Titanium: Inorganic & Coordination Chemistry," p. 4206. Wiley, Chichester, 1994.
49. Müller, C. A., Maciejewski, M., Mallat, T., and Baiker, A., in preparation.